Heliyon 10 (2024) e27153

Contents lists available at ScienceDirect

Heliyon

journal homepage: www.cell.com/heliyon

Research article

Exploring the functional role of tRF-39-8HM2OSRNLNKSEKH9 in hepatocellular carcinoma

Tianxin Xu [a,1], Jie Yuan [b,1], Fei Song [a], Nannan Zhang [a], Cheng Gao [a], Zhong Chen [a,*]

[a] *Department of General Surgery, Affiliated Hospital of Nantong University, Medical School of Nantong University, Nantong, China*
[b] *Department of Laboratory Medicine, Affiliated Hospital of Nantong University, Medical School of Nantong University, Nantong, China*

A R T I C L E I N F O

Keywords:
Hepatocellular carcinoma
tRNA-derived small RNAs
Oncogene
Proliferation
Migration
Invasion

A B S T R A C T

Hepatocellular carcinoma (HCC) is associated with high morbidity and mortality globally. tRNA-derived small RNAs (tsRNAs) have emerged as potential targets for cancer treatment. However, the specific impact of tsRNAs on HCC remains undiscovered. In this study, we aimed to investigate the biological significance of tsRNAs in HCC. First, we screened the differentially expressed tsRNAs in HCC tissues and normal tissues adjacent to the tumor (NAT) using high-throughput sequencing and the results showed that tRF-39-8HM2OSRNLNKSEKH9 was more highly expressed in HCC tissues than NATs. Agarose gel electrophoresis (AGE), nuclear-cytoplasmic separation assays and fluorescence in situ hybridization (FISH) were employed to assess the characterization of tRF-39-8HM2OSRNLNKSEKH9. The relationship between the expression of tRF-39-8HM2OSRNLNKSEKH9 and clinicopathological parameters was evaluated and we found that it was positively associated with tumor size. The cell counting kit-8 (CCK8) assay, colony formation assay and EdU staining assay were employed to investigate the role of tRF-39-8HM2OSRNLNKSEKH9 in the proliferation of HCC cells. Additionally, transwell assays demonstrated that overexpression of tRF-39-8HM2OSRNLNKSEKH9 could accelerate cell migration capability. Taken together, tRF-39-8HM2OSRNLNKSEKH9 was highly expressed in HCC cells, serum and tissues, and it may play an oncogenic role in HCC cells through interacting with downstream mRNA targets.

1. Introduction

Hepatocellular carcinoma (HCC) is currently the sixth most common cancer and the third leading cause of cancer-related death worldwide [1]. Viral hepatitis, particularly viral hepatitis B and viral hepatitis C, is still the most common underlying cause of liver cirrhosis and approximately 80%–90% of patients with cirrhosis develop primary liver cancer [2]. Although the incidence rate of viral hepatitis B and viral hepatitis C has decreased due to comprehensive vaccination, other risk factors, including aflatoxin exposure, alcoholic liver disease, nonalcoholic fatty liver disease (NAFLD), metabolic diseases and so on, are gradually becoming the main cause of HCC worldwide [3,4]. Meanwhile, the accumulation of numerous aberrations and dysregulations of genetic and epigenetic alterations might affect the expression levels of both mRNAs and noncoding RNAs (ncRNAs), eventually contributing to both

* Corresponding author.Department of General Surgery, Affiliated Hospital of Nantong University, Medical School of Nantong University, 20 Xisi Road, Nantong, 226001, Jiangsu Province, China.
E-mail address: chenzhong_nt@163.com (Z. Chen).
[1] Tianxin Xu and Jie Yuan are co-first authors and contributed equally to this work.

https://doi.org/10.1016/j.heliyon.2024.e27153
Received 29 July 2023; Received in revised form 14 February 2024; Accepted 26 February 2024
Available online 27 February 2024
2405-8440/

tumorigenicity and the invasive behavior of HCC [5]. Therefore, it is necessary to further explore new functional genes and clarify potential molecular mechanisms to develop new therapeutic drugs and improve the prognosis of patients with HCC.

ncRNAs are a group of single-stranded RNAs that lack an open coding framework and cannot be translated into proteins. With the cutting-edge technology of next-generation sequencing, an increasing number of ncRNAs have been identified, including miRNAs, lncRNAs, piRNAs, circRNAs, tsRNAs, etc., which are involved in diverse physiological and pathological processes [6,7]. Among them, researchers have rarely focused on tRNA-derived small RNAs (tsRNAs). tsRNAs consist of tRNA-derived small fragments (tRFs) and tRNA halves (tiRNAs), which are cleaved under conditions of stress such as hypoxia, oxidative stress, heat shock and nutritional deficiency [8]. In addition, tRFs include 1-tRF, 3-tRF, 5-tRF, and 2-tRF (also known as i-tRF) and tiRNAs include 5′-tiRNA and 3′-tiRNA according to their specific cleavage site of premature tRNAs or mature tRNAs by the ribonuclease family such as angiogenin (ANG), Dicer, or other RNases [9]. In 1979, Borek et al. found first high levels of tsRNAs in urine of patients with urogenital tumors which quickly returned to normal after effective chemotherapy [10]. Currently, the roles of tsRNAs are gradually becoming clear to scientists because of their abundant expression [11]. Due to their stability in serum, recent studies have shown that some tsRNAs could serve as novel biomarkers in some types of cancers. For example, Wang et al. revealed that six tRFs from the 5′ ends of tRNAs were significantly downregulated in plasma samples of patients with early-stage breast cancers [12]. Wang et al. first analyzed tsRNA signatures in systemic lupus erythematosus (SLE) serum and identified that tRF-His-GTG-1 was significantly upregulated in SLE serum [13]. They also found that serum tRF-Pro-AGG-004 and tRF-Leu-CAG-002 could be used as novel promising biomarkers for pancreatic cancer (PC) diagnosis and play a tumor-promoting role in PC [14].

In addition to being a valuable noninvasive biomarker, tsRNAs could play diverse biological roles through different mechanisms including gene silencing, protein-binding abilities, ribosome biogenesis, RNA processing, and oncogenic formation, and are associated with proliferation, migration, and invasion in some types of cancer [8,15–19]. For example, Kay et al. demonstrated that inhibition of 3′tsRNA-LeuCAG, which binds at least two ribosomal protein mRNAs, induces apoptosis both *in vitro* and in patient-derived orthotopic hepatocellular carcinoma model in mice [15]. Yan et al. found that 5′-tiRNA-Val could act as a new tumor-suppressor through inhibition of the FZD3/Wnt/β-Catenin signaling pathway, which could act as a potential diagnostic biomarker for breast cancer [17]. In lung carcinoma, tsRNA-5001a was found to be significantly upregulated and could increase the risk of postoperative recurrence and poor prognosis [20].

In this study, by employing Arraystar Human tRF&tiRNA sequencing technology, we performed a comprehensive analysis of tsRNA expression profiles and successfully identified a group of tsRNAs that exhibited differential expression in HCC tissues compared with normal liver tissues. The expression level of tRF-39-8HM2OSRNLNKSEKH9, which is abbreviated as 'tRF-39-8HM' in this article, was first measured in HCC patients who were newly diagnosed. Then, their association with clinicopathological characteristics was analyzed statistically in an attempt to provide insights into the potential diagnostic or prognostic assessment. Thereafter, the influence of tRF-39-8HM on HCC cell lines was confirmed through cell phenotypic assays. Additionally, bioinformatics analysis was employed to predict the target genes of tRF-39-8HM.

In conclusion, there is compelling evidence to suggest that tRF-39-8HM can exert an oncogenic role in HCC and that the detection of tRF-39-8HM may hold potential as a diagnostic tool or as a target for therapeutic interventions in HCC.

2. Materials and methods

2.1. Tissue and serum samples

We obtained 48 paired HCC tissues and their normal tissues adjacent to the tumor (NAT) from the Affiliated Hospital of Nantong University (Nantong, Jiangsu, China). Tissue specimens were immediately preserved in MACS Tissue Storage Solution (Miltenyi Biotec, Germany) after removal from the patients and kept at −80 °C until further use. Meanwhile, serum samples, including sera from 70 HCC patients and another 70 healthy donors, were obtained from the Clinical Laboratory of the Affiliated Hospital of Nantong University, and 48 operation patients mentioned above are included within 70 HCC patients in this group. None of the patients had received radiotherapy, chemotherapy, targeted therapy or immune therapy before surgery. Written informed consent was obtained from each patient in this study. The study protocol was approved by the ethics committee of the Affiliated Hospital of Nantong University (ethical review report number: 2018-L006). All the investigations were carried out in accordance with the rules of the declaration of Helsinki of 1975.

2.2. tsRNA sequencing and expression analysis

Arraystar Human tRF&tiRNA PCR Array technology was employed to analyze 3 pairs of HCC and adjacent normal tissues. Purified total RNA samples were extracted from 3 paired HCC tissues and tumor-adjacent normal tissues. Because some RNA modifications could interfere with small RNA-seq library construction or RT-PCR, the rtStar™ tRF&tiRNA Pretreatment Kit (#: AS–FS–005, Arraystar, MD, USA) was used to remove 3′-aminoacyl, 3′-cP, phosphorylate 5′-OH, and demethylate m1A, m1G, and m3C for efficient cDNA reverse transcription [21]. Then, the rtStar™ tRF&tiRNA First-Strand cDNA Synthesis Kit (#: AS–FS–003, Arraystar, MD, USA) was used to establish cDNA libraries following sequential 3′ and 5′ adaptor ligation. The complete libraries were determined by means of an Agilent 2100 Bioanalyzer using an Agilent DNA 1000 chip kit (#: 5067-1504, Agilent, California, USA) and then sequenced on an Illumina NextSeq 500 system using a NextSeq 500/550 V2 kit (#: FC-404-2005, Illumina) according to the manufacturer's instructions. The abundance of tsRNAs was evaluated using their sequencing counts and was normalized as counts per million (CPM) of total aligned reads. The expression profiling and differentially expressed tsRNAs were analyzed and calculated using R packages

(EdgeR 3.32.1) [22]. Finally, the sequencing reads were aligned to mature-tRNA on the entire genome using MINTbase v2.0, a database for the interactive exploration of mitochondrial and nuclear tRNA fragments.

2.3. Cell lines

HCC cell lines (HepG2, HuH-7, HCCLM3, SK-Hep-1, PCL/PRF/5, Hep3B) were obtained from SIBCB (Shanghai Institute of Biochemistry and Cell Biology, Shanghai, China) and Beyotime Biotechnology (Shanghai, China). Human immortalized hepatocytes (THLE-2) were purchased from ATCC (CRL-2706™). Resource Identification Initiative ID (RRID) for each cell lines are shown in Supplementary file 1. HepG2, HuH-7, HCCLM3, and PCL/PRF/5 cells were cultivated in high-glucose DMEM (GIBCO). SK-Hep-1 and Hep3B cells were cultured in MEM (Invitrogen) supplemented with GlutaMAX, NEAA (nonessential amino acids) and sodium pyruvate. THLE-2 cells were cultivated in BEGM BulletKit medium (Lonza). All media were supplemented with 10% fetal bovine serum (FBS) (GIBCO) and 1% penicillin-streptomycin (Pen/Strep) mixture (HyClone, Logan, UT, USA) and deposited at 37 °C with 5% CO_2.

2.4. RNA extraction, reverse transcription and quantitative real-time PCR

Total RNA in tissue and cell samples was isolated via the TRIzol RNA Extraction Kit (Invitrogen, Carlsbad, CA, USA), purified by 75% ethanol and suspended by DEPC-treated water. Serum total RNA was extracted via the Total RNA Pure and Isolation Kit with rotating column (BioTeke, Beijing, China). Then, RNA concentration and purity were determined by taking OD measurements at 260 nm and 280 nm and the OD 260/280 absorbance ratio was between 1.8 and 2.1. To quantify the amount of tsRNAs, cDNA was synthesized from nearly 500 ng of RNA. cDNA was amplified by Revert Aid RT Reverse Transcription Kit (Thermo Fisher Scientific, USA) in a total of 10 μl, which was incubated at 42 °C for 1 h and then inactivated at 70 °C for 5 min qPCR reaction condition includes an initial step of 10 min at 95 °C to activate the chemically modified hot-start DNA polymerase, normally followed by 35 cycles of a 10-s denaturation at 95 °C and then 60 s annealing and extension at 60 °C. All steps were performed following the manufacturer's instructions. qRT-PCR was performed with the FastStart Universal SYBR Green Master Mix (Roche, Mannheim, Germany) on a QuantStudio 5 (Thermo, Waltham, MA, USA) in a reaction system of 20 μl, including 10 μl of SYBR Green I Mix, 5 μl of cDNA, 1 μl of primer, and 3 μl of enzyme-free water. RNU6B (U6) was used as an internal control to standardize the relative expression of tRF-39-8HM. All primers used in this study were synthesized by RiboBio Corporation (Guangzhou, China). Subsequently, the $2^{-\Delta\Delta Ct}$ method was utilized to analyze the resulting relative expression level data [23]. The ΔΔCt value was expressed as the difference between the experimental group ($Ct^{target} - Ct^{reference}$) and the control group ($Ct^{target} - Ct^{reference}$).

2.5. Agarose gel electrophoresis (AGE) assay

Agarose gel electrophoresis assay was used to evaluate PCR reaction success. 6 μL DNA marker or 1 μL DNA samples mixed with 5 μL DNA loading buffer (6X) (Beyotime Biotechnology, Shanghai, China) were separated using 2% agarose gel electrophoresis. The DNA Ladder (500bp Plus Marker, NO. C500233, Sangon Biotech, Shanghai, China) consists of 8 liner double stranded DNA bands of 50, 100, 150, 200, 250, 300, 400 and 500 base pair and the intensity of 250 bp band has been increased to yield reference indicator. The DNA fragments on the gel were visualized using gel imaging system (ChemiDoc™ MP, Bio-Rad Laboratories, Inc. USA).

2.6. Nuclear-cytoplasmic separation assay

The cellular localization of tRF-39-8HM was assessed by a nuclear-cytoplasmic separation assay. Nuclear and cytoplasmic RNA was isolated from HCCLM3 and SK-Hep-1 cell lines using a PARIST™ kit according to the manufacturer's protocol (Invitrogen, Thermo Fisher Scientific, USA). Then, the RNA expression of tsRNAs in the nucleus and cytoplasm was measured by qRT-PCR. U6 and GAPDH were used as nuclear and cytoplasmic references, respectively.

2.7. Fluorescence in situ hybridization (FISH)

FISH assays were conducted to visualize the localization of tRF-39-8HM in HCC cells. Cy3-labeled tRF-39-8HM probes were synthesized by Servicebio Technology Co., Ltd. (Wuhan, China). The hybridization process was carried out using the Fluorescent In Situ Hybridization Kit following the manufacturer's instructions. Nuclei were counterstained with 4,6-diamidino-2-phenylindole (DAPI) (Beyotime Biotechnology, Shanghai, China). Images were captured using a fluorescence microscope from Olympus (Tokyo, Japan).

Table 1
RNA sequences used for RNA interference.

Name	RNA sequence
Mimics	5′-UCACGCGGGAGACCGGGGUUCGAUUCCCCGACGGGGAGC-3′
Mimic Negative control	5′-UUUGUACUACACAAAAGUACUG-3′
Inhibitor	5′-GCUCCCCGUCGGGGAAUCGAACCCCGGUCUCCCGCGUGA-3′
Inhibitor Negative control	5′-CAGUACUUUUGUGUAGUACAAA-3′

2.8. RNA interference and transfection

The tRF-39-8HM mimics/inhibitor and their negative control (NC) mimics/inhibitor were obtained from Ribobio (Guangzhou RiboBio Co., Ltd.) and were transfected using Lipofectamine 3000 (Invitrogen) reagent in 6-well plates according to the manufacturer's protocols. The RNA sequences of mimics/inhibitor and NC are shown in Table 1. Cells were seeded into 6-well plates overnight before transfection. The transfection concentration of the tRF-39-8HM mimics is 50 nM, while the concentration of the tRF-39-8HM inhibitor is 100 nM. After transfection for 48 h, the cells were collected to assess the expression of tRF-39-8HM using qRT-PCR. After transfection overnight, the cells were subjected to cellular phenotypic assays.

2.9. CCK8 assay

For the cell proliferation assay, CCK8 (Cell Counting Kit-8) was utilized to detect the function of cell behavior. For the CCK8 assay, treated cells were seeded on 96-well plates at a density of 3×10^3 cells per well and cultured for 1–5 days. Each well was incubated with 100 μL of complete culture medium (10% FBS). Ten microliters of CCK-8 detection solution (Code: CK04, Dojindo Laboratories, Japan) was added in each well and incubated for 2 h. OD_{450} was measured using a microplate reader (TECAN-Spark, Switzerland).

2.10. Colony formation assay

For the colony formation assay, 1×10^3 cells were seeded in 2 mL of complete culture medium in a 6-well plate for 14 days. After 2 weeks, colonies were fixed with 4% paraformaldehyde solution and then stained using crystal violet. The number of cell clones was counted using ImageJ software v1.47 (NIH, USA) [24].

2.11. EdU staining assay

Based on the protocols of the supplier, the CellorLab™ EdU Cell Proliferation Kit with Alexa Fluor 555 (Epizyme, Shanghai, China) was utilized to implement this assay. Approximately 5×10^5 cells in 6-well plates were cultured in complete medium with a concentration of 10 μM EdU and incubated for 2 h at 37 °C with 5% CO_2. After metabolic labeling, cells in each well were fixed using 3.7% formaldehyde and then permeabilized using 0.5% Triton™ X-100 (Sigma−Aldrich, Saint Louis, USA). Under dark conditions, the samples were stained with Alexa Fluor 555 for 30 min. DAPI was used to stain cells for 10 min. Finally, the cells were observed via fluorescence microscopy (Olympus, Tokyo, Japan).

2.12. Transwell migration assay

For migration ability, cells were digested with trypsin-EDTA after 48 h of transfection. Then, the cell suspension was seeded into the Transwell upper chamber (Corning Inc., Costar®, USA). Then, 100 μL cell solution containing 5×10^4 cells in serum-free medium was plated on top of the filter membrane in the upper chamber and 500 μL of medium containing 10% (v/v) FBS was added to the lower chamber. Cells were cultured at 37 °C with 5% CO_2 for 24 h. The next day, nonmigrated cells in the upper chamber were removed with a cotton-tipped applicator, and the cells on the lower surface of the Transwell inserts were fixed and stained with 0.2% crystal violet. The number of migrated cells on the underside of the inserts was quantified using ImageJ software v1.47.

2.13. GO and KEGG enrichment analysis

GO (Gene Oncology) function analysis and KEGG (Kyoto Encyclopedia of Genes and Genomes) pathway analysis were enriched and generated by the website https://www.bioinformatics.com.cn (last accessed on Nov 10, 2023), an online platform for data analysis and visualization.

2.14. Statistical analysis

All data were analyzed with SPSS 24.0 statistical software (IBM SPSS Statistics, Chicago, USA) and GraphPad PRISM 8.0 (GraphPad Software, San Diego, CA, USA). Student's *t*-test was used to analyze the differences between two groups. Pearson's chi-squared test was utilized to evaluate the correlation between tRF-39-8HM and clinicopathological factors in HCC. Data are presented as the mean ± standard deviation (SD). For the analysis of survival data, Kaplan–Meier curves were constructed, and the log-rank test was performed. Differences were considered statistically significant at $P < 0.05$. All experiments were performed in triplicate in order to ensure the robustness and reliability of the results.

3. Results

3.1. Expression of tRF-39-8HM2OSRNLNKSEKH9 in HCC tissues and serum

First, the study flow chart is presented in Fig. 1. The bioinformatic results showed that there were 2401 expressed tsRNAs in total and we screened 358 significantly differentially expressed tsRNAs ($p < 0.05$ and $|Log2FC|>1.5$), of which 161 tsRNAs (shown in

Supplementary file 2) were upregulated and 197 were downregulated. The heatmap of these differentially expressed tsRNAs is shown in Fig. 2A, and the volcano plot is illustrated in Fig. 2B. Among 161 upregulated tsRNAs, 70 intersected with 221 tsRNAs uniquely expressed in tumors (shown in Fig. 2C). The top 5 upregulated and downregulated tsRNAs are shown in Fig. 2D. To further validate the results of the tRF&tiRNA sequencing data, the top 5 tsRNAs with the greatest differences were selected as candidates, and were examined in additional 3 pairs of tumors and corresponding adjacent normal tissues. Notably, the results showed that significantly higher levels of tRF-39-8HM were detected in tumors than in adjacent normal specimens (shown in Fig. 2E) and were basically consistent with the sequencing results. This finding was further confirmed using qRT-PCR in 48 pairs of HCC specimens and the statistical analysis results showed that tRF-39-8HM was upregulated in human HCC tissues (shown in Fig. 2F). Then, we divided the 48 HCC patients into two groups based on their sera median expression level of tRF-39-8HM: a relatively high-expression group (expression level > median, n = 24) and a relatively low-expression group (expression level ≤ median, n = 24). To evaluate the correlation between tRF-39-8HM expression and clinicopathological parameters in these 48 HCC patients, we used either the chi-square test or Fisher's exact test. The analysis demonstrated a significant correlation between the expression level of tRF-39-8HM and tumor size ($P < 0.05$), while no statistically significant associations were observed with other parameters, including age, sex, HBV infection, level of AFP, tumor multiplicity, MVI (microvascular invasion), and BCLC (Barcelona Clinic Liver Cancer) stage (Table 2). These findings suggested that the increased expression of tRF-39-8HM may have underlying value in predicting the malignant growth of tumors. Consistently, we detected the relative expression of serum tRF-39-8HM in 70 HCC patients compared to that in 70 healthy donors, and the results showed that tRF-39-8HM was highly expressed in HCC patients (shown in Fig. 2G). In addition, Kaplan–Meier analysis for 70 HCC patients revealed that high tRF-39-8HM expression was significantly correlated with shorter overall survival (shown in Fig. 2H; $P < 0.05$). Given that there was a lack of specific research on this newly discovered tsRNA, our research was centered around tRF-39-8HM as a crucial molecule that we believe plays a significant role in the progression of HCC.

3.2. *Brief introduction and characteristics of tRF-39-8HM2OSRNLNKSEKH9*

To date, there are two main types of tsRNAs: tRNA halves, also known as tiRNAs (5′-tiRNA and 3′-tiRNA), and tRFs (1-tRF, 3-tRF, 5-tRF and i-tRF). In the MINTbase v2.0 database (http://cm.jefferson.edu/MINTbase/), tRF-39-8HM2OSRNLNKSEKH9 has a length of 39 nt (5′-TCACGCGGGAGACCGGGGTTCGATTCCCCGACGGGGAGC-3′) and is classified into 3′-tiRNA, which owns 3′-half of the mature tRNA-Asp-GTC (shown in Fig. S1A). The cleavage sites are indicated with red scissors symbols according to the online database tRNAdb (http://trna.bioinf.uni-leipzig.de/) (shown in Fig. S1B). In addition, to test the accuracy of the products of qRT-PCR, nucleic acids and oligonucleotides were separated using agarose gel electrophoresis (AGE) assay, we detected a single electrophoresis band approximately 80 bp in size (shown in Fig. 3A). Additionally, we found that tRF-39-8HM had smooth amplification curves and single-peak melting curves (shown in Fig. 3B). Finally, to assess the intracellular localization of tRF-39-8HM in HCCLM3 and SK-Hep-1 cell lines, both nuclear-cytoplasmic separation assays and FISH staining assays were used to demonstrate that tRF-39-8HM was mainly located in the cytoplasm in the indicated cell lines (shown in Fig. 3C and D).

3.3. *tRF-39-8HM2OSRNLNKSEKH9 plays an oncogenic role in HCC*

To investigate the biological role of tRF-39-8HM in HCC cell lines, we initially examined the relative expression in different HCC cell lines. As shown in Fig. 4A, HCCLM3 cells exhibited the highest expression level of tRF-39-8HM, while SK-Hep-1 cell line was the

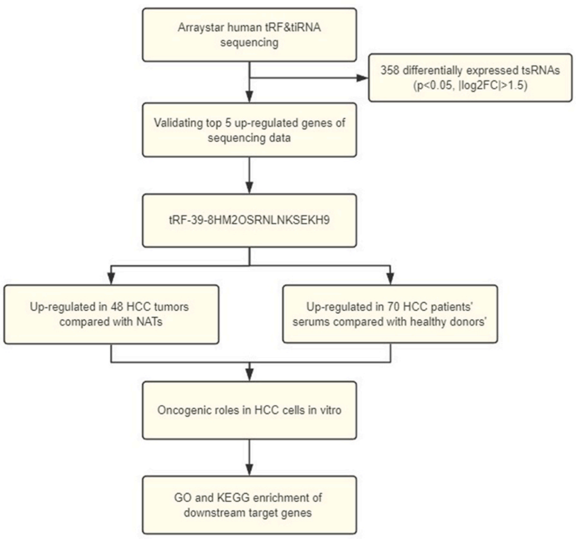

Fig. 1. Flow chart of the study.

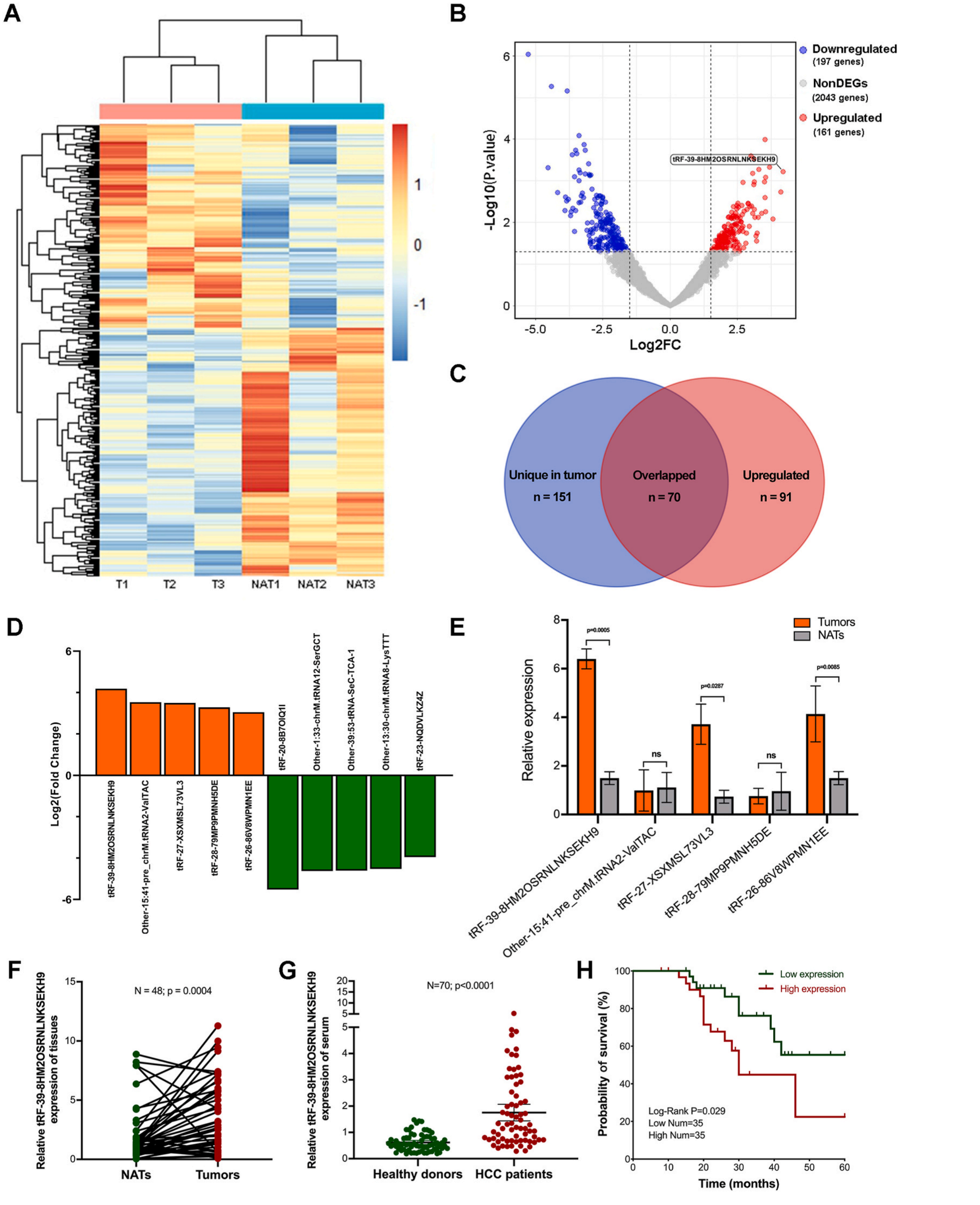

Fig. 2. Expression profiles of tsRNAs in HCC and the screening of tRF-39-8HM2OSRNLNKSEKH9. A. Heatmap displaying differentially expressed tsRNAs between three pairs of HCC tumors and corresponding NATs by the R package edgeR ($p < 0.05$ and $|Log2FC|>1.5$). **B.** Volcano plots of upregulated and downregulated tsRNAs. **C.** Diagram of overlapping genes between upregulated genes and genes unique to tumors. **D.** Top 5 upregulated and downregulated genes in tumor tissues relative to NATs. **E.** Validating the relative expression levels of the top 5 upregulated tsRNAs in HCC tumors and NATs. **F.** The relative expression levels of tRF-39-8HM in 48 pairs of HCC patients. **G.** The relative expression levels of serum tRF-39-8HM in HCC patients compared to healthy donors. U6 was used for normalization. **H.** Kaplan–Meier survival curves for 70 HCC patients according to tRF-39-8HM expression status. *Indicated statistical significance (****$P < 0.0001$, ***$P < 0.001$, **$P < 0.01$, *$P < 0.05$); NS, no significance.

Table 2
The association between tRF-39-8HM2OSRNLNKSEKH9 expression and clinicopathologic parameters in 48 HCC surgical specimens.

Clinical pathological indexes	HCC tissues		Total (n = 48)	χ^2	*P*-value
	tRF-39-8HM low expression (n = 24, ≤ median)	tRF-39-8HM high expression (n = 24, >median)			
Age (years)				0.751	0.386
≥ 60	14	11	25		
< 60	10	13	23		
Gender				0.343	0.558
Male	13	15	28		
Female	11	9	20		
HBV infection				0.091	0.763
Positive	15	16	31		
Negative	9	8	17		
AFP (ng/ml)				0.087	0.768
≤ 20	10	9	19		
> 20	14	15	29		
Tumor size				4.269	0.039*
≤ 3 cm	11	18	29		
> 3 cm	13	6	19		
Tumor multiplicity				0.356	0.551
Single	23	22	45		
Multiple	1	2	3		
MVI				1.091	0.296
MVI 0	23	21	44		
MVI 1 + 2	1	3	4		
BCLC Stage				2.087	0.1486
Stage 0+A	24	22	46		
Stage B	0	2	2		

AFP, Alpha-Fetoprotein; MVI, Microvascular Invasion; BCLC, Barcelona Clinic Liver Cancer.

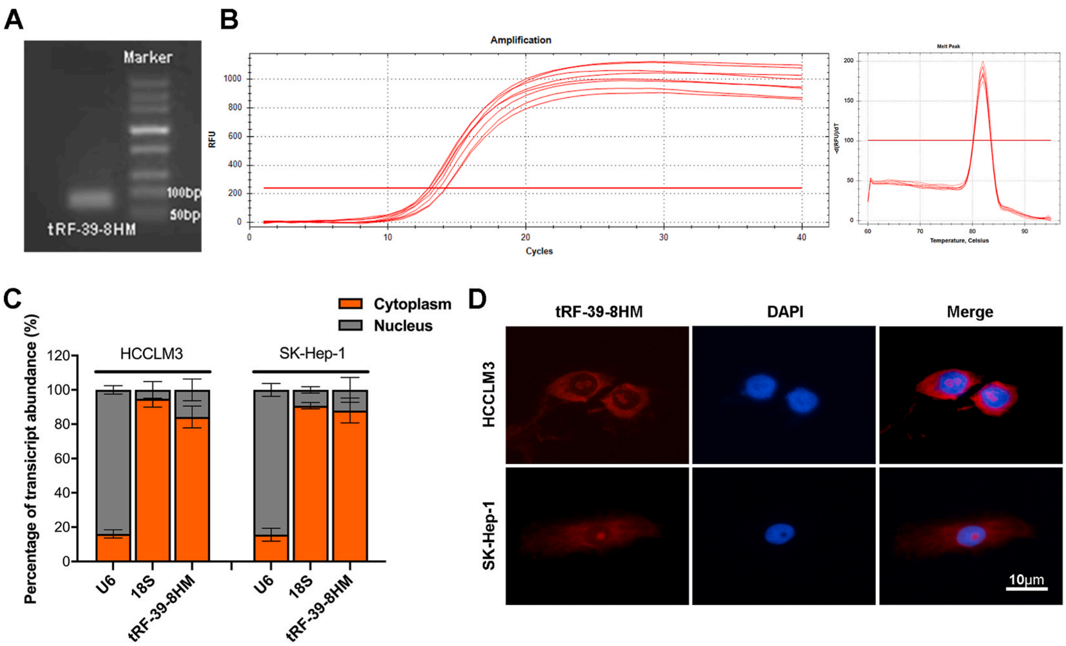

Fig. 3. Characteristics of tRF-39-8HM2OSRNLNKSEKH9. A. The qRT-PCR product was subjected to electrophoresis on a 2.5% agarose gel, which displayed a single band with an approximate size of 80 bp (The uncropped version was shown in Fig. S2). **B.** Smooth amplification curves (left) and single-peak melting curves (right) of tRF-39-8HM. **C.** A nuclear-cytoplasmic separation assay was used to assess the intracellular localization of tRF-39-8HM in HCCLM3 and SK-Hep-1 cell lines. **D.** FISH assay was used to visualize the localization of tRF-39-8HM in HCCLM3 and SK-Hep-1 cell lines.

least upregulated cell line compared with the normal liver cell line. Subsequently, we conducted transfection experiments using tRF-39-8HM mimics and their negative control (M − NC), as well as a tRF-39-8HM inhibitor and its negative control (I-NC), in both HCCLM3 and SK-Hep-1 cells. The efficiency of tRF-39-8HM mimics and inhibitors was assessed using qRT-PCR. The results showed that the expression of tRF-39-8HM mimics in HCCLM3 cells was 28-fold higher than that in M − NCs, while in SK-Hep-1 cells, it was tenfold higher than that in M − NCs (shown in Fig. 4B). To examine the impact of tRF-39-8HM on cell proliferation, CCK-8 assays were performed and the results revealed that the overexpression of tRF-39-8HM significantly enhance cell proliferation compared to that in the M − NC group. Conversely, the knockdown of tRF-39-8HM exhibited the opposite effects in comparison with the I-NC group, indicating a decrease in cell proliferation (shown in Fig. 4C). Similarly, the colony formation assay provided further evidence that the overexpression of tRF-39-8HM enhanced the capacity of single-cell growth, and conversely, the knockdown group exhibited a marked inhibition of cell growth, indicating a suppressive effect of tRF-39-8HM on colony formation (shown in Fig. 4D and E). Additionally, we performed EdU staining to evaluate the proportion of proliferating cells. The results demonstrated that the inhibition of tRF-39-8HM led to a decrease in the ratio of EdU-positive cells, whereas overexpression of tRF-39-8HM reversed this effect, resulting in an increased

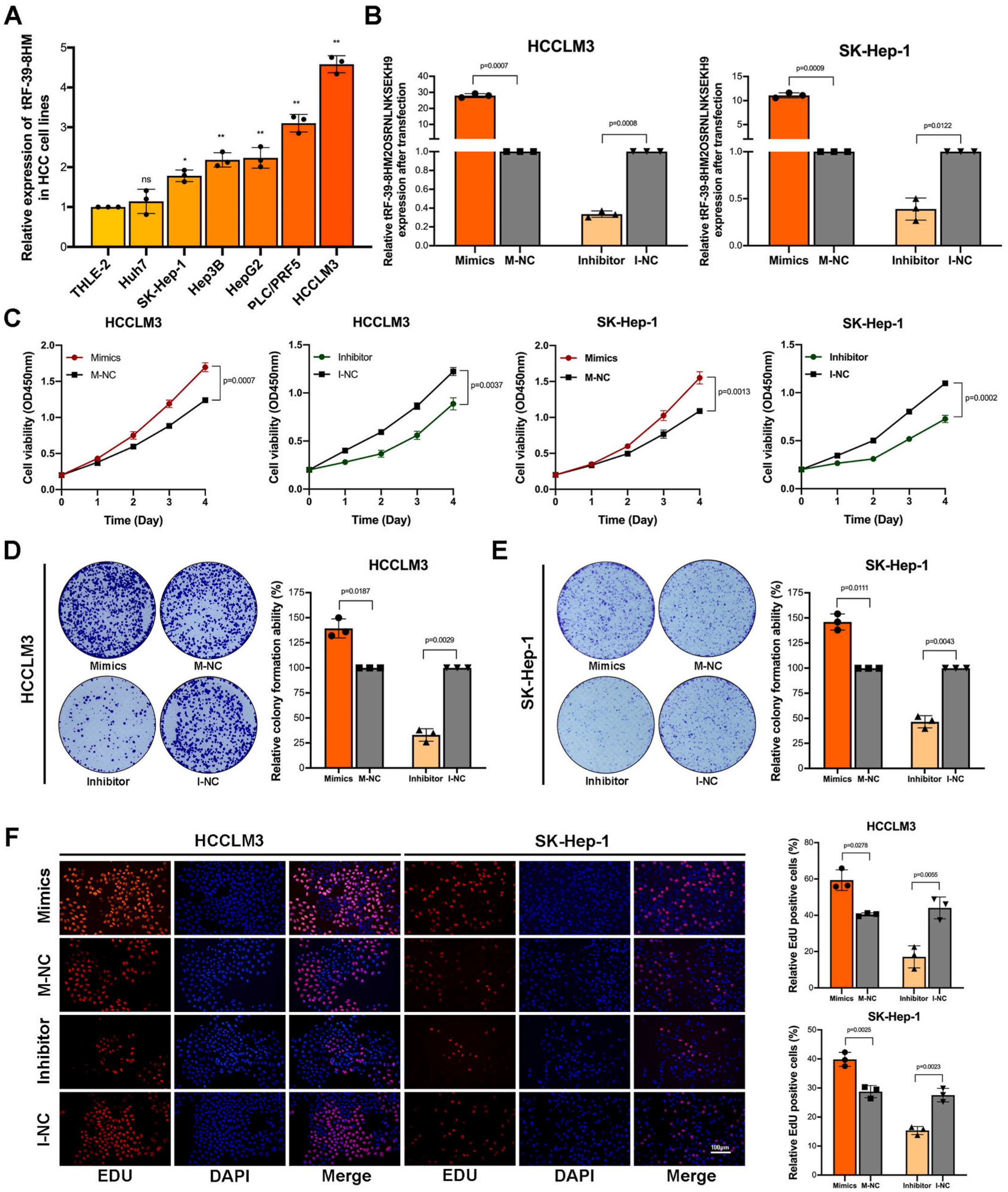

Fig. 4. tRF-39-8HM2OSRNLNKSEKH9 promoted the proliferation of HCC cells *in vitro*. A. Relative expression of tRF-39-8HM in HCC cells. **B.** The efficiency of tRF-39-8HM mimics and inhibitor in both HCCLM3 and SK-Hep-1 cell lines was evaluated using qRT-PCR. **C.** The cell viability of HCC cell lines was assessed following transfection with mimics or a negative control (NC) by CCK-8 assay. **D and E.** Colony formation assays were used to determine the effect of tRF-39-8HM on cell growth and the relative colony formation ability (%) was calculated using ImageJ software. **F.** EdU staining was used to evaluate the proportion of proliferating cells in both HCCLM3 and SK-Hep-1 cells after transfection.

proportion of EdU-positive cells (shown in Fig. 4F). Furthermore, we conducted Transwell assays to investigate the potential involvement of tRF-39-8HM in tumor cell migration and invasion. The results revealed that overexpression of tRF-39-8HM in both HCCLM3 and SK-Hep-1 cells accelerated cell migration and invasion abilities compared to that in the M − NC group, whereas knockdown of tRF-39-8HM significantly decreased cell migration and invasion abilities (Fig. 5). Collectively, the obtained results strongly suggest that tRF-39-8HM may serve as an oncogenic driver in the carcinogenesis of HCC.

3.4. GO and KEGG enrichment analysis of tRF-39-8HM target genes

We reasoned that tsRNAs could participate in cancer progression analogous to certain miRNAs [25]. Therefore, to explore the molecular function of tRF-39-8HM, we employed multiple bioinformatics tools, including miRanda, TargetScan, miRWalk, and miRDB, to predict potential target genes and their corresponding binding sites. This collective approach allowed us to identify potential downstream targets of tRF-39-8HM. The analysis of overlapping results (generated using jvenn: an interactive Venn diagram viewer) from the above four database prediction tools revealed a total of 702 potential target genes that exhibited a high likelihood of binding to tRF-39-8HM (shown in Fig. 6A, Supplementary file 3). GO function analysis and KEGG pathway analysis were enriched and generated by the website bioinformatics.com.cn and could provide a systematic approach to understanding the functional implications of the target genes at the molecular, cellular, and pathway levels. The enrichment of GO function analysis encompassed three categories: biological process (BP), cellular component (CC), and molecular function (MF). As shown in Fig. 6B, GO enrichment analysis revealed potential roles of tRF-39-8HM in various biological processes, such as positive regulation of cellular catabolic processes, regulation of lipid biosynthetic processes, Ras GTPase binding, etc. In addition, Sankey dot pathway enrichment was used to analyze

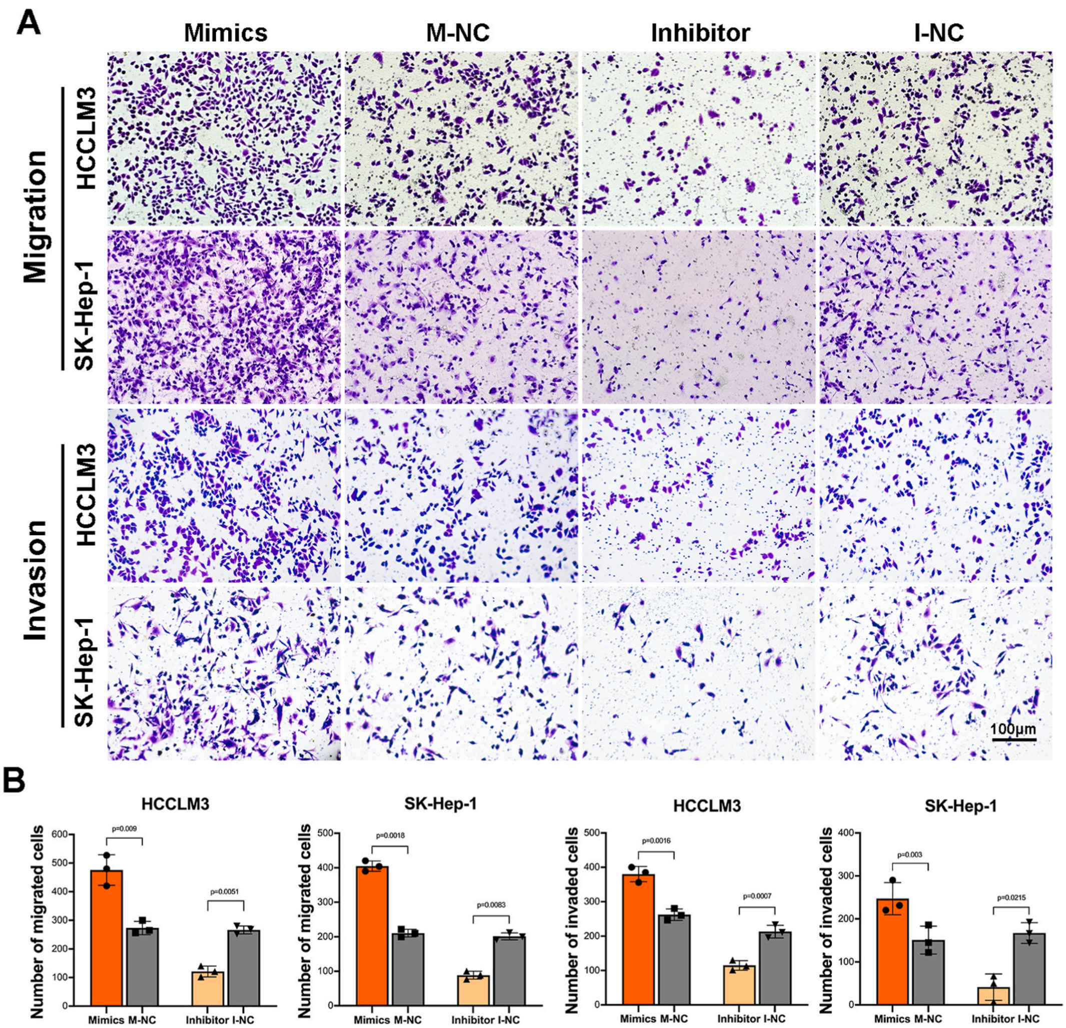

Fig. 5. tRF-39-8HM2OSRNLNKSEKH9 could accelerate cell migration and invasion abilities. A. Cell migration and invasion assays were performed after transfection of tRF-39-8HM mimics/M − NC and inhibitor/I-NC in HCCLM3 and SK-Hep-1 cell lines. **B.** Corresponding bar graphs were depicted to investigate the migration and invasion abilities of HCCLM3 and SK-Hep-1 cell lines.

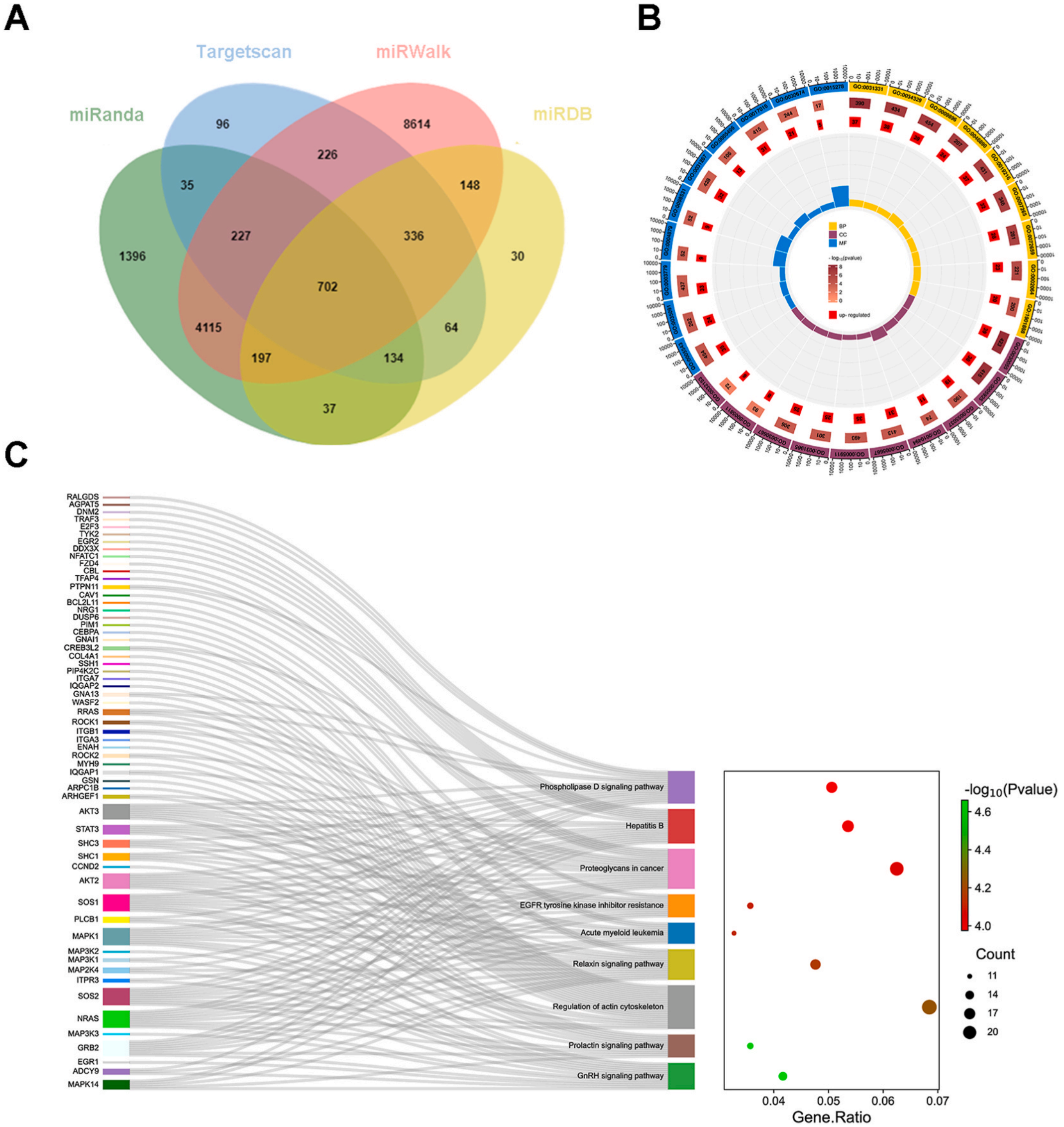

Fig. 6. GO and KEGG enrichment analyses of tRF-39-8HM2OSRNLNKSEKH9 target genes. A. Schematic diagram of tRF-39-8HM target prediction. Venn diagram evaluating the overlapping genes among miRanda, TargetScan, miRWalk and miRDB. **B.** GO circle analysis of the tRF-39-8HM target genes enriched in biological process, cellular component, and molecular function. **C.** Sankey dot pathway enrichment was used to analyze the enrichment of KEGG signaling pathways, and the related genes involved in the corresponding pathways are listed.

the enrichment of KEGG signaling pathways, and the results suggested that the phospholipase D signaling pathway, hepatitis B, proteoglycans in cancer, EGFR tyrosine kinase inhibitor resistance, cellular senescence, etc., were significantly enriched, and the related genes involved in the corresponding pathways are listed (shown in Fig. 6C). These results indicated that tRF-39-8HM may play an important role in the occurrence and development of HCC by targeting downstream mRNAs, which could open up a new avenue for further exploration of the specific molecular mechanisms of tRF-39-8HM2OSRNLNKSEKH9.

4. Discussion

While recognizing the advancements made in the realm of cancer diagnosis and treatment, hepatocellular carcinoma (HCC) is still the main cause of primary liver cancer and one of the most prevalent fatal cancers in the world. Although surgical techniques, radiotherapy, chemotherapy drugs, targeted therapy, and immunotherapy have progressed, the overall prognosis remains unsatisfactory and the mortality of HCC still ranks second worldwide [1]. Over the last few years, explosive advances in next-generation sequencing technology have enabled the evaluation of clinical settings and enhanced our comprehensive understanding of the molecular mechanism of tumorigenesis. As technology develops, new types of small cancer-associated noncoding RNAs are decrypted in different cells, sera and tissues. As one of the most abundant small RNA entities, tRNAs and their derivatives, which take part in the pathogenic process of cancer, have attracted broad attention [26]. An increasing number of studies have reported that tsRNAs contribute to the occurrence and development of diverse cancers such as pancreatic cancer [14], breast cancer [27], non-small cell lung cancer [28], and colorectal cancer [29], etc. In addition, many studies have indicated that serum tsRNA could serve as a novel biomarker for the diagnosis of HCC. Zhan et al. identified that serum mitochondrial tRF-Gln-TTG-006 had a high sensitivity and specificity at the early stage of HCC [30]. In addition, Yi Zuo et al. applied a diagnostic model to develop a tsRNA-based risk score signature for liver cancer prognosis, and the results showed that the expression of tRF-20-HDK2RSI2, tRF-20-6S7P4PZ3, and tRF-18-8R1546D2 were upregulated while the expression of tRF-20-73VL4YMY and tRF-24-S3M8309N0Y were downregulated in HCC tissue [31]. However, the in-depth exploration of the underlying mechanisms of tsRNAs in HCC is still in its early stages.

In the present study, we used the Arraystar Human tRF&tiRNA sequencing technology to analyze differentially expressed tsRNAs in HCC tissue compared with the normal tissues adjacent to the tumor. This advanced technology facilitated comprehensive profiling and detection of tsRNAs in the samples. Specifically, some tsRNAs were found to be upregulated in HCC, suggesting a potential role in promoting HCC development. Conversely, other tsRNAs were downregulated, indicating a potential tumor-suppressive function. Our data confirmed that tRF-39-8HM was markedly upregulated in 3 pairs of HCC tissues. Then, further analysis of 48 surgical specimens from HCC patients helped determine whether there was a significant relationship between tRF-39-8HM expression and the clinicopathological characteristics of the HCC patients and we observed that the relatively high tRF-39-8HM expression group had a significantly larger tumor size in HCC patients. Based on this result, cell proliferation assays were conducted comprehensively. Similarly, we conducted an analysis to determine the relative expression of serum tRF-39-8HM in patients diagnosed with HCC in comparison to healthy individuals. The findings of this study revealed a significant upregulation of tRF-39-8HM in HCC patients.

Subsequently, the biological functions of tRF-39-8HM were explored in this study. To demonstrate its impact on cell proliferation, several experimental techniques were employed, including CCK8 assay, colony formation assay, and EdU staining assay. The gain-of-function experiment of tRF-39-8HM in HCC cell lines revealed that the overexpression of tRF-39-8HM resulted in a substantial enhancement in cell proliferation, whereas the loss-of-function experiment demonstrated that the inhibition of tRF-39-8HM could significantly suppress tumor cell proliferation. Additionally, overexpression of tRF-39-8HM also led to an increase in migration and invasion abilities. In summary, these results strongly indicated that tRF-39-8HM could play an oncogenic role in the development of HCC.

miRNAs typically bind to the 3′-UTR of mRNAs, leading to mRNA degradation or translational repression. Similarly, tsRNAs can interact with mRNA targets, affecting their stability or translation [27]. Due to its miRNA-like functions, we performed predictions to identify potential downstream mRNA targets of tRF-39-8HM. By delving deeper into the interactions between tRF-39-8HM and its target genes and exploring the associated signaling pathways, we can gain a better understanding of the precise molecular mechanisms by which tRF-39-8HM influences HCC. GO enrichment analysis suggested that tRF-39-8HM might be involved in important cellular processes and molecular interactions related to catabolism, lipid biosynthesis, Ras signaling, etc. KEGG enrichment analysis indicated that several pathways were significantly enriched, including the phospholipase D signaling pathway, hepatitis B, proteoglycans in cancer, EGFR tyrosine kinase inhibitor resistance, and cellular senescence. By elucidating the downstream mRNA targets, further exploration can be undertaken to investigate the intricate molecular mechanisms, as well as the signaling cascades and regulatory networks involved.

However, it is important to acknowledge that our original study had several limitations. First, the three pairs of HCC tissues and NATs used for sequencing, as well as the sera of the HCC patients and healthy donors, were taken from a homogenous population from Affiliated Hospital of Nantong University. Specimens from multiregional clinical centers should be collected for in-depth research and analysis. In addition, the majority of the candidate HCC patients were diagnosed with HBV-related disease rather than nonalcoholic fatty liver disease (NAFLD). Therefore, the clinical data in this study could not encompass all differentially expressed tsRNAs. Second, some tsRNAs have been reported to serve as diagnostic biomarkers for specific types of cancers such as breast cancer [32], gastric cancer [33], and pancreatic cancer [34]. However, the sequencing data in this study were derived from the tissues of HCC patients, and whether tRF-39-8HM could be utilized as a novel serum biomarker has yet to be determined. Thus, it may be worth considering conducting serum-based tRF&tiRNA sequencing, which could overlap with the histological sequencing data, followed by comprehensive bioinformatic analysis. Last, but not least importantly, an increasing number of studies have indicated that tsRNAs could influence downstream factors through gene silencing or protein-binding abilities. Because tRF-39-8HM is located in the cytoplasm as per the results of the nuclear-cytoplasmic separation assay and FISH, we speculate that tRF-39-8HM might play a part in the post-transcriptional regulation of HCC through miRNA-like functions. Thus, further studies, such as RNA pull-down, luciferase reporter assays, or RNA immunoprecipitation, are needed to investigate whether tRF-39-8HM can interact with its target mRNAs to affect the onset and progression of HCC.

Above all, these findings shed light on the involvement of tRF-39-8HM in HCC and provide valuable insights into its potential as a diagnostic or therapeutic target. Further investigations are required to elucidate the precise mechanisms by which tRF-39-8HM could contribute to HCC pathogenesis.

5. Conclusion

The small noncoding RNA molecule tRF-39-8HM2OSRNLNKSEKH9 has been found to be significantly upregulated in HCC cell lines, as well as in serum and tissues associated with HCC. Its increased expression suggested a potential oncogenic role in HCC development. To gain insights into the underlying mechanisms, we conducted downstream target functional enrichments, which were found to be involved in various cellular processes and signaling pathways that were relevant to cancer development and progression.

These findings contributed to a better understanding of the molecular mechanisms underlying HCC and highlighted the potential significance of tRF-39-8HM2OSRNLNKSEKH9 as a therapeutic target in HCC treatment.

Funding

This work was supported by grants from the National Natural Science Foundation of China (No. 81871927) and Postgraduate Research & Practice Innovation Program of Jiangsu Province (KYCX22-3366).

Statement of ethics

This study was performed in line with the principles of the https://www.wma.net/policies-post/wma-declaration-of-helsinki-ethical-principles-for-medical-research-involving-human-subjects/. Klicken oder tippen Sie, wenn Sie diesem Link Vertrauen.">-World Medical Association Declaration of Helsinki (as revised in 2013). Approval was granted by the ethics committee of Affiliated Hospital of Nantong University (ethical review report number: 2018-L006). Written informed consent was obtained from all individual participants included in the study and data was analyzed anonymously.

Data availability statement

Data will be made available on request.

CRediT authorship contribution statement

Tianxin Xu: Writing – original draft, Software, Methodology, Funding acquisition, Conceptualization. **Jie Yuan:** Software, Methodology, Conceptualization. **Fei Song:** Data curation, Conceptualization. **Nannan Zhang:** Visualization, Investigation, Conceptualization. **Cheng Gao:** Data curation, Conceptualization. **Zhong Chen:** Writing – review & editing, Supervision, Funding acquisition, Conceptualization.

Declaration of competing interest

The authors declare that they have no known competing financial interests or personal relationships that could have appeared to influence the work reported in this paper.

Appendix A. Supplementary data

Supplementary data to this article can be found online at https://doi.org/10.1016/j.heliyon.2024.e27153.

References

[1] H. Sung, J. Ferlay, R.L. Siegel, M. Laversanne, I. Soerjomataram, A. Jemal, F. Bray, Global cancer Statistics 2020: GLOBOCAN estimates of incidence and mortality worldwide for 36 cancers in 185 countries, Ca - Cancer J. Clin. 71 (3) (2021) 209–249.
[2] M. Wu, H. Miao, R. Fu, J. Zhang, W. Zheng, Hepatic stellate cell: a potential target for hepatocellular carcinoma, Curr. Mol. Pharmacol. 13 (4) (2020) 261–272.
[3] P. Konyn, A. Ahmed, D. Kim, Current epidemiology in hepatocellular carcinoma, Expet Rev. Gastroenterol. Hepatol. 15 (11) (2021) 1295–1307.
[4] J.D. Yang, P. Hainaut, G.J. Gores, A. Amadou, A. Plymoth, L.R. Roberts, A global view of hepatocellular carcinoma: trends, risk, prevention and management, Nat. Rev. Gastroenterol. Hepatol. 16 (10) (2019) 589–604.
[5] M. Kanda, H. Sugimoto, Y. Kodera, Genetic and epigenetic aspects of initiation and progression of hepatocellular carcinoma, World J. Gastroenterol. 21 (37) (2015) 10584–10597.
[6] S. Bhogireddy, S.K. Mangrauthia, R. Kumar, A.K. Pandey, S. Singh, A. Jain, H. Budak, R.K. Varshney, H. Kudapa, Regulatory non-coding RNAs: a new frontier in regulation of plant biology, Funct. Integr. Genomics 21 (3–4) (2021) 313–330.
[7] A.F. Palazzo, E.S. Lee, Non-coding RNA: what is functional and what is junk? Front. Genet. 6 (2015) 2.
[8] Q. Chen, X. Zhang, J. Shi, M. Yan, T. Zhou, Origins and evolving functionalities of tRNA-derived small RNAs, Trends Biochem. Sci. 46 (10) (2021) 790–804.
[9] X. Li, X. Liu, D. Zhao, W. Cui, Y. Wu, C. Zhang, C. Duan, tRNA-derived small RNAs: novel regulators of cancer hallmarks and targets of clinical application, Cell Death Dis. 7 (1) (2021) 249.
[10] J. Speer, C.W. Gehrke, K.C. Kuo, T.P. Waalkes, E. Borek, tRNA breakdown products as markers for cancer, Cancer 44 (6) (1979) 2120–2123.
[11] Y. Pekarsky, V. Balatti, C.M. Croce, tRNA-derived fragments (tRFs) in cancer, J. Cell Commun. Signal 17 (1) (2023) 47–54.
[12] J. Wang, G. Ma, M. Li, X. Han, J. Xu, M. Liang, X. Mao, X. Chen, T. Xia, X. Liu, S. Wang, Plasma tRNA fragments derived from 5' ends as novel diagnostic biomarkers for early-stage breast cancer, Mol. Ther. Nucleic Acids 21 (2020) 954–964.
[13] P. Yang, X. Zhang, S. Chen, Y. Tao, M. Ning, Y. Zhu, J. Liang, W. Kong, B. Shi, Z. Li, H. Shen, Y. Wang, A novel serum tsRNA for diagnosis and prediction of nephritis in SLE, Front. Immunol. 12 (2021) 735105.
[14] F. Jin, L. Yang, W. Wang, N. Yuan, S. Zhan, P. Yang, X. Chen, T. Ma, Y. Wang, A novel class of tsRNA signatures as biomarkers for diagnosis and prognosis of pancreatic cancer, Mol. Cancer 20 (1) (2021) 95.
[15] H.K. Kim, G. Fuchs, S. Wang, W. Wei, Y. Zhang, H. Park, B. Roy-Chaudhuri, P. Li, J. Xu, K. Chu, F. Zhang, M.S. Chua, S. So, Q.C. Zhang, P. Sarnow, M.A. Kay, A transfer-RNA-derived small RNA regulates ribosome biogenesis, Nature 552 (7683) (2017) 57–62.
[16] E.W. Tao, H.L. Wang, W.Y. Cheng, Q.Q. Liu, Y.X. Chen, Q.Y. Gao, A specific tRNA half, 5'tiRNA-His-GTG, responds to hypoxia via the HIF1alpha/ANG axis and promotes colorectal cancer progression by regulating LATS2, J. Exp. Clin. Cancer Res. 40 (1) (2021) 67.

[17] D. Mo, P. Jiang, Y. Yang, X. Mao, X. Tan, X. Tang, D. Wei, B. Li, X. Wang, L. Tang, F. Yan, A tRNA fragment, 5'-tiRNA(Val), suppresses the Wnt/beta-catenin signaling pathway by targeting FZD3 in breast cancer, Cancer Lett. 457 (2019) 60–73.
[18] D. Liu, C. Wu, J. Wang, L. Zhang, Z. Sun, S. Chen, Y. Ding, W. Wang, Transfer RNA-derived fragment 5'tRF-Gly promotes the development of hepatocellular carcinoma by direct targeting of carcinoembryonic antigen-related cell adhesion molecule 1, Cancer Sci. 113 (10) (2022) 3476–3488.
[19] H. Goodarzi, X. Liu, H.C. Nguyen, S. Zhang, L. Fish, S.F. Tavazoie, Endogenous tRNA-derived fragments suppress breast cancer progression via YBX1 displacement, Cell 161 (4) (2015) 790–802.
[20] F. Hu, Y. Niu, X. Mao, J. Cui, X. Wu, C.B. Simone 2nd, H.S. Kang, W. Qin, L. Jiang, tsRNA-5001a promotes proliferation of lung adenocarcinoma cells and is associated with postoperative recurrence in lung adenocarcinoma patients, Transl. Lung Cancer Res. 10 (10) (2021) 3957–3972.
[21] C. Cosentino, S. Toivonen, E. Diaz Villamil, M. Atta, J.L. Ravanat, S. Demine, A.A. Schiavo, N. Pachera, J.P. Deglasse, J.C. Jonas, D. Balboa, T. Otonkoski, E. R. Pearson, P. Marchetti, D.L. Eizirik, M. Cnop, M. Igoillo-Esteve, Pancreatic beta-cell tRNA hypomethylation and fragmentation link TRMT10A deficiency with diabetes, Nucleic Acids Res. 46 (19) (2018) 10302–10318.
[22] M.D. Robinson, D.J. McCarthy, G.K. Smyth edgeR, A Bioconductor package for differential expression analysis of digital gene expression data, Bioinformatics 26 (1) (2010) 139–140.
[23] K.J. Livak, T.D. Schmittgen, Analysis of relative gene expression data using real-time quantitative PCR and the 2(-Delta Delta C(T)) Method, Methods 25 (4) (2001) 402–408.
[24] C.A. Schneider, W.S. Rasband, K.W. Eliceiri, NIH Image to ImageJ: 25 years of image analysis, Nat. Methods 9 (7) (2012) 671–675.
[25] J. Krol, I. Loedige, W. Filipowicz, The widespread regulation of microRNA biogenesis, function and decay, Nat. Rev. Genet. 11 (9) (2010) 597–610.
[26] J. Li, L. Zhu, J. Cheng, Y. Peng, Transfer RNA-derived small RNA: a rising star in oncology, Semin. Cancer Biol. 75 (2021) 29–37.
[27] Z. Zhang, Z. Liu, W. Zhao, X. Zhao, Y. Tao, tRF-19-W4PU732S promotes breast cancer cell malignant activity by targeting inhibition of RPL27A (ribosomal protein-L27A), Bioengineered 13 (2) (2022) 2087–2098.
[28] W. Yang, K. Gao, Y. Qian, Y. Huang, Q. Xiang, C. Chen, Q. Chen, Y. Wang, F. Fang, Q. He, S. Chen, J. Xiong, Y. Chen, N. Xie, D. Zheng, R. Zhai, A novel tRNA-derived fragment AS-tDR-007333 promotes the malignancy of NSCLC via the HSPB1/MED29 and ELK4/MED29 axes, J. Hematol. Oncol. 15 (1) (2022) 53.
[29] S. Lu, X. Wei, L. Tao, D. Dong, W. Hu, Q. Zhang, Y. Tao, C. Yu, D. Sun, H. Cheng, A novel tRNA-derived fragment tRF-3022b modulates cell apoptosis and M2 macrophage polarization via binding to cytokines in colorectal cancer, J. Hematol. Oncol. 15 (1) (2022) 176.
[30] S. Zhan, P. Yang, S. Zhou, Y. Xu, R. Xu, G. Liang, C. Zhang, X. Chen, L. Yang, F. Jin, Y. Wang, Serum mitochondrial tsRNA serves as a novel biomarker for hepatocarcinoma diagnosis, Front. Med. 16 (2) (2022) 216–226.
[31] Y. Zuo, S. Chen, L. Yan, L. Hu, S. Bowler, E. Zitello, G. Huang, Y. Deng, Development of a tRNA-derived small RNA diagnostic and prognostic signature in liver cancer, Genes. Dis. 9 (2) (2022) 393–400.
[32] Y. Zhang, Z. Bi, X. Dong, M. Yu, K. Wang, X. Song, L. Xie, X. Song, tRNA-derived fragments: tRF-Gly-CCC-046, tRF-Tyr-GTA-010 and tRF-Pro-TGG-001 as novel diagnostic biomarkers for breast cancer, Thorac. Cancer 12 (17) (2021) 2314–2323.
[33] Y. Zhang, X. Gu, X. Qin, Y. Huang, S. Ju, Evaluation of serum tRF-23-Q99P9P9NDD as a potential biomarker for the clinical diagnosis of gastric cancer, Mol. Med. 28 (1) (2022) 63.
[34] M. Xue, M. Shi, J. Xie, J. Zhang, L. Jiang, X. Deng, C. Peng, B. Shen, H. Xu, H. Chen, Serum tRNA-derived small RNAs as potential novel diagnostic biomarkers for pancreatic ductal adenocarcinoma, Am. J. Cancer Res. 11 (3) (2021) 837–848.